

- [3] G. Hilmersson, Ö. Davidsson, *J. Org. Chem.* **1995**, *60*, 7660–7669.
- [4] G. Hilmersson, P. I. Arvidsson, Ö. Davidsson, M. Håkansson, *Organometallics* **1997**, *16*, 3352–3362; G. Hilmersson, P. I. Arvidsson, Ö. Davidsson, M. Håkansson, *J. Am. Chem. Soc.* **1998**, *120*, 8143–8149; P. I. Arvidsson, G. Hilmersson, P. Ahlberg, *J. Am. Chem. Soc.* **1999**, *121*, 1883–1887; H. J. Reich, B. Ö. Gudmundsson, *J. Am. Chem. Soc.* **1996**, *118*, 6074–6075; H. J. Reich, D. P. Green, M. A. Medina, W. S. Goldenberg, B. Ö. Gudmundsson, R. R. Dykstra, N. H. Phillips, *J. Am. Chem. Soc.* **1998**, *120*, 7201–7210; J. S. DePue, D. B. Collum, *J. Am. Chem. Soc.* **1988**, *110*, 5518–5524; B. L. Lucht, D. B. Collum, *J. Am. Chem. Soc.* **1996**, *118*, 2217–2225; B. L. Lucht, M. P. Bernstein, J. F. Remenar, D. B. Collum, *J. Am. Chem. Soc.* **1996**, *118*, 10707–10718.
- [5] T. Koizumi, K. Morihashi, O. Kikuchi, *Bull. Chem. Soc. Jpn.* **1996**, *69*, 305–309.
- [6] F. E. Romesberg, J. H. Gilchrist, A. T. Harrison, D. J. Fuller, D. B. Collum, *J. Am. Chem. Soc.* **1991**, *113*, 5751–5757.
- [7] R. F. Schmitz, F. J. J. de Kanter, M. Schakel, G. W. Klumpp, *Tetrahedron* **1994**, *50*, 5933–5944.
- [8] We are grateful to one of the referees for drawing our attention to this point and plan to investigate this remarkable observation in a full paper. For a review on the transfer of chirality, see H. Buschmann, H.-D. Scharf, N. Hofmann, P. Esser, *Angew. Chem.* **1991**, *103*, 480–518; *Angew. Chem. Int. Ed. Engl.* **1991**, *30*, 477–515, and references therein.
- [9] Note added in proof: In a recent paper Collum's group also attributed a change in ^{16}Li , ^{15}N coupling constant to a solution change. K. B. Aubrecht, B. L. Lucht, D. B. Collum, *Organometallics* **1999**, *18*, 2981–2987.

Low-Temperature, Catalyzed Growth of Indium Nitride Fibers from Azido-Indium Precursors**

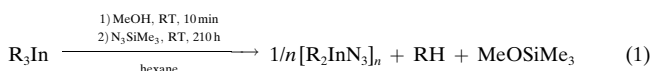
Sean D. Dingman, Nigam P. Rath, Paul D. Markowitz, Patrick C. Gibbons, and William E. Buhro*

We have achieved low-temperature synthesis and crystallization of InN through precursor design and crystal-growth catalysis. The group III nitrides GaN, InN, $\text{In}_n\text{Ga}_{1-n}\text{N}$, and $\text{Al}_n\text{Ga}_{1-n}\text{N}$ have recently acquired technological importance for blue/violet LED and laser diode applications.^[1] However, InN begins decomposing with loss of N_2 at low temperatures (427–550°C),^[2,3] which makes the growth of crystalline InN-containing materials challenging. We now report, to our knowledge, the lowest-temperature synthesis of crystalline

InN, at 203°C, well below its decomposition range. The work demonstrates that catalysis effectively lowers crystallization barriers, allowing InN synthesis under the mild conditions of conventional, solution-phase chemistry. Catalyzed growth may thus offer new strategies for the preparation of crystalline, thermally unstable materials.

Typical chemical vapor deposition (CVD)^[2] and melt^[3] syntheses of InN and InN-containing alloys require temperatures within or above the InN decomposition range, and proceed with difficulty. Recently, crystalline InN has been grown by single-source CVD at the surprisingly low temperature of 350°C.^[4] Efforts to prepare covalent, nonmolecular solids like InN at such low temperatures generally produce only amorphous products, due to the lack of active crystal-growth mechanisms.^[5] We now report that InN crystal growth is activated at 203°C by a process in which nanometer-sized metal droplets serve as catalytic sites for crystalline fiber formation. The growth process appears to be directly analogous to the previously reported solution–liquid–solid (SLS) mechanism (see below).^[5,6]

Azido precursor compounds have been previously used for CVD of group III nitrides;^[2a,b,4,7] we have developed appropriate analogs for low-temperature, solution-phase growth of InN. The precursors $i\text{Pr}_2\text{InN}_3$ (**1a**) and $t\text{Bu}_2\text{InN}_3$ (**1b**) were prepared in one-pot procedures from the corresponding trialkylindanes via dialkylmethoxyindane intermediates [Eq. (1); R = *i*Pr (**1a**), *t*Bu (**1b**); 85–95% yields]. The



products are effectively insoluble in hydrocarbons at room temperature, but dissolve in Lewis-basic solvents such as pyridine and acetone. In the solid state, **1a** and **1b** are isostructural, ladderlike polymers (Figure 1).^[8]

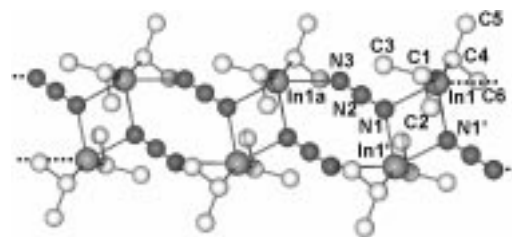


Figure 1. Ball-and-stick representation of the crystal structure of $[i\text{Pr}_2\text{InN}_3]_n$ (**1a**).^[8] Selected bond distances [Å] and angles [°]: In1–C1 2.166(2), In1–N1 2.296(2), In1–N1' 2.433(1), In1a–N3 2.655(3), N1–N2 1.194(2), N2–N3 1.138(3); C4–In1–C1 147.26(8), C1–In1–N1 105.21(7), C1–In1–N1' 99.07(7), In1–N1–In1' 107.66(6), C5–C4–In1 112.55(18), C4–In1–N1' 97.82(7), N1–In1–N1' 72.34(6), N3–N2–N1 178.9(2).

Reactions of the precursors **1a** or **1b** with the mild reductant^[9] 1,1-dimethylhydrazine, H_2NNMe_2 , produced crystalline InN. Thermolysis of **1a** in refluxing diisopropylbenzene (203°C) without H_2NNMe_2 gave a gray-black precipitate with a broad powder X-ray diffraction (XRD) pattern (Figure 2a), indicating an amorphous structure. However, thermolysis of **1a** under the same conditions but with H_2NNMe_2 gave black InN having an average XRD coherence length (approximate

[*] Prof. W. E. Buhro, S. D. Dingman, P. D. Markowitz
Department of Chemistry
Washington University
St. Louis, MO 63130-4899 (USA)
Fax: (+1) 314-935-4481
E-mail: buhro@wuchem.wustl.edu

Dr. N. P. Rath
Department of Chemistry and Center for Molecular Electronics
University of Missouri–St. Louis
St. Louis, MO 63121 (USA)
Prof. P. C. Gibbons
Department of Physics
Washington University
St. Louis, MO 63130-4899 (USA)

[**] This work was supported by the U.S. National Science Foundation (Grant CHE-9709104). We gratefully acknowledge assistance from Dr. W. R. Winchester with GC-MS and Dr. Couture with X-ray fluorescence studies.

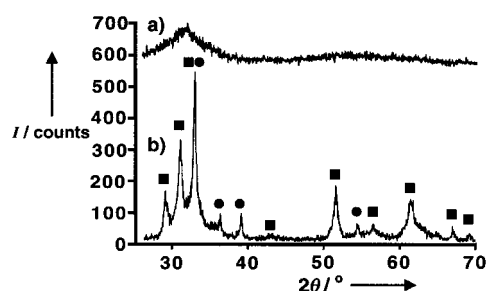
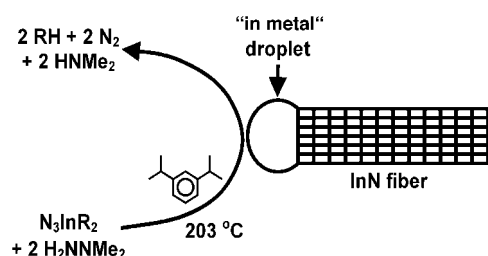


Figure 2. Powder X-ray diffraction patterns of InN formed by solution-state thermolysis of **1a** at 203°C a) in the absence of and b) in the presence of 1,1-dimethylhydrazine. ■ InN reflections, ● In reflections.

crystallite dimension) of 18 nm (Figure 2b), as determined by the Scherrer equation.^[10] Refined lattice parameters $a = 3.551(6)$ Å and $b = 5.754(12)$ Å were extracted from the XRD data, which compared well to the literature values of $a = 3.537$ Å and $b = 5.704$ Å for InN.^[11] Reflections for metallic indium were also evident in the XRD pattern; elemental analysis established a InN:In molar ratio of 80:20. Thermolysis of **1b** with H_2NNMe_2 gave similar results. Thermolysis of **1b** without H_2NNMe_2 also gave crystalline InN, although the XRD coherence length was smaller (12 nm versus 7 nm, with and without H_2NNMe_2), and the crystallite morphologies of the two samples were very different (see below). Monitoring of the H_2NNMe_2 reactions by NMR and GC-MS, which detected the alkane and HNMe_2 byproducts, suggested the process shown in Scheme 1.



Scheme 1. Proposed solution-liquid-solid (SLS) growth mechanism for InN synthesis from the dialkyl(azido)indane precursors N_3InR_2 **1a** or **1b**.

Polycrystalline InN fibers, of diameters around 20 nm and lengths in the range 100–1000 nm, predominated transmission electron microscope (TEM) images of the materials produced in the H_2NNMe_2 reactions, as is evident in Figure 3. The fiber diameters were consistent with the coherence lengths from the XRD. No features suggestive of amorphous byproducts were found in the images. Each InN fiber exhibited a metallic indium droplet attached to its tip. Energy dispersive X-ray spectroscopy on the fiber in Figure 3c gave In:N ratios of 60(5):40(5) and 45(5):54(5) at two locations along the fiber length; only indium was detected in the droplet attached to the fiber tip (see arrow in Figure 3c; nitrogen detection limit was ca. 5%). In contrast, the dominant morphology obtained from thermolysis of **1b** without 1,1-dimethylhydrazine was small (< 10 nm), equidimensional InN nanocrystallites; only a very small fraction (< 2%) of stunted InN fibers with indium droplets was present.

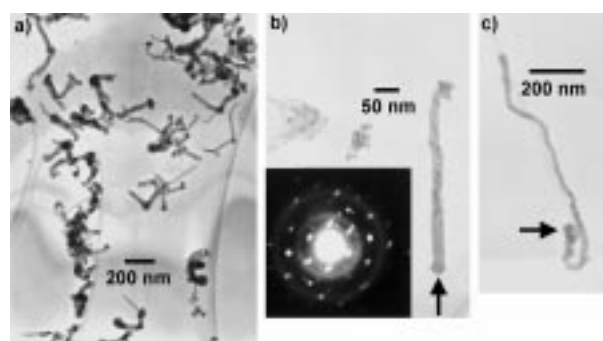


Figure 3. Representative TEM images of InN produced according to Scheme 1 show that fibrous morphologies are formed almost exclusively: a) and b) from precursor **1a**; c) from precursor **1b**. The inset in b) is an electron-diffraction pattern collected from the fiber in image b); the intense spots index to the (033) zone of InN and indicate the whisker axis aligns with the (210) direction of this primary crystal grain. Faint spots due to secondary, misaligned InN crystal grains are also evident. The rings in the inset index to reflections of randomly oriented metallic indium. Arrows indicate metallic indium droplets attached to InN fiber tips; many such droplets are also evident in image a).

A primary role of H_2NNMe_2 (Scheme 1) was as a stoichiometric hydrogen-atom donor to assist alkane elimination. Other potential hydrogen donors PhSH, Me_2NH , and PhNH_2 were not effective in promoting InN fiber growth. Note that the N–N bond in H_2NNMe_2 was cleaved and N_2 was generated, which is likely to provide a driving force for hydrogen donation. Because N_2 and/or N were generated, one must consider that 1,1-dimethylhydrazine may also serve as a nitrogen atom donor to InN. However, reactions of $t\text{Bu}_3\text{In}$ and H_2NNMe_2 under these conditions gave only amorphous products and metallic indium, strongly suggesting that H_2NNMe_2 was not a primary nitrogen donor. Thus, the N_3 ligand was implicated as the nitrogen source. 1,1-Dimethylhydrazine also induced metallic indium generation, discussed below.

Fiber growth was observed only when indium was also generated. Indium droplets were observed to form in the presence of H_2NNMe_2 , but not in the absence of a hydrogen-atom donating coreactant. Thus, H_2NNMe_2 is a sufficiently strong reductant^[9] to convert some of **1a** or **1b** to metallic indium under the reaction conditions. If indium formation had occurred in a process subsequent and unrelated to fiber growth, then the droplets would have been indiscriminately distributed on and about the fibers. Since the indium droplets were found *only* at the fiber tips and not in other configurations, these observations strongly suggest that the indium droplets formed in an adventitious side reaction preceding InN fiber growth,^[6b] and performed a catalytic role in fiber growth.

Metal droplets catalyze whisker and fiber growth under higher-temperature CVD conditions in a process known as the vapor-liquid-solid (VLS) mechanism.^[12] A solution-phase analog of the VLS mechanism, the SLS mechanism, was recently elucidated.^[6a] In both VLS and SLS growth, the catalytic droplets promote both precursor decomposition and crystal-lattice construction as shown in Scheme 1.^[5, 6] The principal requirements established for the catalytic metal is that it be molten under the reaction conditions and that at

least one constituent of the product has a limited solubility in it. Under our reaction conditions, indium metal (m.p. 157°C) is indeed molten and dissolves less than 0.001 atomic % nitrogen.^[13] The most obvious characteristics of the VLS^[12] and SLS^[5, 6] mechanisms—one-dimensional fiber or whisker growth morphologies and attached metal-catalyst particles—were clearly evident in the InN samples produced. Consequently, all the key indicators of the SLS growth mechanism were present.

The SLS growth process has been previously demonstrated for group III element phosphides and arsenides,^[5, 6] which are thermally stable at conventional growth temperatures. However, indium nitride is not. The SLS mechanism operates at very low temperatures in comparison to conventional materials-synthesis methods, presumably because it is catalytic and lowers energy barriers for both precursor decomposition and the interfacial steps required for nonmolecular crystal growth (crystal lattice assembly). SLS synthesis of other thermally unstable compounds and crystal structures should be possible.

Experimental Section

Compounds $t\text{Bu}_3\text{In}^{[14]}$ and $i\text{Pr}_3\text{In}^{[15]}$ were prepared according to the literature. The synthesis of $t\text{Bu}_3\text{InN}_3$ (**1b**) is described here; $i\text{Pr}_3\text{InN}_3$ (**1a**) was prepared similarly. MeOH (225 μL , 0.178 g, 5.55 mmol) was added to a dry, O_2 -free solution of $t\text{Bu}_3\text{In}$ (1.61 g, 5.63 mmol) in hexane (20 mL) at 25°C. The mixture was stirred for 10 min and then N_3SiMe_3 (0.800 mL, 0.660 g, 5.73 mmol) was added, instantly generating a fine white precipitate. The slurry was stirred for 2 h. Precursor **1b** was then collected by filtration and washed with 2×5 mL of hexane (yield: 1.39 g, 5.12 mmol, 91 %). Analytical data for **1b**: m.p. 210°C (dec.); elemental analysis calcd for $\text{C}_8\text{H}_{18}\text{InN}_3$: C 35.45, H 6.69, N 15.50; found: C 35.74, H 6.46, N 15.44; ^1H NMR ($[\text{D}_6]\text{acetone}$): $\delta = 1.29$ (s, 18H); IR (KBr): $\tilde{\nu} = 2087\text{ cm}^{-1}$ (asym. N_3). Analytical data for **1a**: m.p. 181°C; ^1H NMR ($[\text{D}_5]\text{pyridine}$): $\delta = 1.34$ (d, 12H, $J = 6.6\text{ Hz}$), 1.45 (m, 2H); IR (KBr): $\tilde{\nu} = 2075\text{ cm}^{-1}$ (asym. N_3). In a typical InN synthesis, **1a** or **1b** (1.5 mmol) and 1,1-dimethylhydrazine (3.0 mmol) were combined in dry, O_2 -free 1,3-diisopropylbenzene (10 mL) at 25°C. The mixture was stirred for 2 h, then heated to reflux at 203°C (in a sand bath under an efficient condenser) for 20 h. The resulting, air-stable InN/In product was collected by filtration and washed with 2×10 mL of pentane (yield: 90–95 %). Elemental analysis calcd for InN: C 0, H 0, N 10.88, In 89.13; found (from **1a**): C 1.87, H 0.12, N 7.31, In 84.1; found (from **1b**): C 2.05, H 0.19, N 8.39, In 81.6.

Received: April 18, 1999

Revised: January 17, 2000 [Z13328]

- [1] a) T. Matsuoka, *Adv. Mater.* **1996**, *8*, 469–479; b) F. A. Ponce, D. P. Bour, *Nature* **1997**, *386*, 351–359; c) S. Nakamura, *Science* **1998**, *281*, 956–961.
- [2] a) D. A. Neumayer, J. G. Ekerdt, *Chem. Mater.* **1996**, *8*, 9–25; b) A. C. Jones, C. R. Whitehouse, J. S. Roberts, *Chem. Vap. Deposition* **1995**, *1*, 65–74; c) I. Akasaki, H. Amano, *J. Crystal Growth* **1995**, *146*, 455–461.
- [3] I. Grzegory, J. Jun, M. Bockowski, St. Krukowski, M. Wróblewski, B. Lucznik, S. Porowski, *J. Phys. Chem. Solids* **1995**, *56*, 639–647.
- [4] R. A. Fischer, A. Miehr, T. Metzger, E. Born, O. Ambacher, H. Angerer, R. Dimitrov, *Chem. Mater.* **1996**, *8*, 1356–1359.
- [5] W. E. Buhro, K. H. Hickman, T. J. Trentler, *Adv. Mater.* **1996**, *8*, 685–688.
- [6] a) T. J. Trentler, K. M. Hickman, S. C. Goel, A. M. Viano, P. C. Gibbons, W. E. Buhro, *Science* **1995**, *270*, 1791–1794; b) T. J. Trentler, S. C. Goel, K. M. Hickman, A. M. Viano, M. Y. Chiang, A. M. Beatty, P. C. Gibbons, W. E. Buhro, *J. Am. Chem. Soc.* **1997**, *119*, 2172–2181.

- [7] a) J. Kouvetakis, D. B. Beach, *Chem. Mater.* **1989**, *1*, 476–478; b) K.-L. Ho, K. F. Jensen, J.-W. Hwang, W. L. Gladfelter, J. F. Evans, *J. Crystal Growth* **1991**, *107*, 376–380.
- [8] Crystallographic data for **1a**: $\text{C}_{12}\text{H}_{28}\text{In}_2\text{N}_6$, monoclinic, space group $P2_1/c$, $a = 8.1680(4)$, $b = 17.6617(10)$, $c = 6.8694(4)$ Å, $\beta = 102.689(4)^\circ$, $V = 966.78(9)$ Å³, $Z = 2$, 22 463 reflections collected, 2405 unique, final $R_1(F) = 0.0184$, final $R_w(F^2) = 0.0446$ for 147 parameters, max./min. residual electron density = $0.70/-0.81\text{ e Å}^{-3}$. Crystallographic data for **1b**: $\text{C}_8\text{H}_{18}\text{InN}_3$, triclinic, space group $P\bar{1}$, $a = 6.8686(1)$, $b = 9.5258(1)$, $c = 9.9383(1)$ Å, $\alpha = 79.536(1)$, $\beta = 85.24$, $\gamma = 70.428(1)^\circ$, $V = 602.32(1)$ Å³, $Z = 2$, 13 486 reflections collected, 2885 unique, final $R_1(F) = 0.0349$, final $R_w(F^2) = 0.0826$ for 109 parameters, max./min. residual electron density = $1.40/-1.16\text{ e Å}^{-3}$. Both data sets were collected using $\text{MoK}\alpha$ radiation ($\lambda = 0.71073$ Å) at 223(2) K with a Bruker SMART CCD Diffractometer. Full matrix refinement was conducted on F^2 and H atoms were refined for **1a**. Details of the X-ray diffraction studies will be published elsewhere. Crystallographic data (excluding structure factors) for the structures reported in this paper have been deposited with the Cambridge Crystallographic Data Centre as supplementary publication no. CCDC-119361 (**1a**) and -119362 (**1b**). Copies of the data can be obtained free of charge on application to CCDC, 12 Union Road, Cambridge CB2 1EZ, UK (fax: (+44) 1223-336-033; e-mail: deposit@ccdc.cam.ac.uk).
- [9] P. A. S. Smith, *Derivatives of Hydrazine and Other Hydronitrogens Having N–N Bonds*, Benjamin/Cummings, Readings, **1983**, p. 20.
- [10] A. R. West, *Solid State Chemistry and its Applications*, Wiley, New York, **1984**, p. 174.
- [11] JCPDS card 02-1450 (indium nitride).
- [12] R. S. Wagner in *Whisker Technology* (Ed.: A. P. Levitt), Wiley, New York, **1970**, chap. 3.
- [13] S. Porowski, I. Grzegory, *EMIS Datarev. Ser.* **1994**, *11*, 82–85.
- [14] D. C. Bradley, D. M. Frigo, M. B. Hursthouse, B. Hussain, *Organometallics* **1988**, *7*, 1112–1115.
- [15] B. Neumueller, *Chem. Ber.* **1989**, *122*, 2283–2287.

Oxidation–Reduction and Photochemical Reactions of Metalladecaborane Clusters: The Interconversion of *hypercloso*- $[(\eta^6\text{-C}_6\text{Me}_6)\text{RuB}_9\text{H}_9]$ and *closo*- $[(\eta^6\text{-C}_6\text{Me}_6)\text{RuB}_9\text{H}_9]^{2-}$

Ralf Littger, Ulrich Englisch, Karin Ruhlandt-Senge, and James T. Spencer*

The most common structure for a 10-vertex polyhedral cluster with a $2n+2$ skeletal electron count (where n is the number of vertices) is the bicapped square antiprism (**I**; Scheme 1).^[1] In one of the two known isomeric forms of these

[*] Prof. J. T. Spencer, R. Littger, U. Englisch, Dr. K. Ruhlandt-Senge
Department of Chemistry and
the W. M. Keck Center for Molecular Electronics
Center for Science and Technology, Syracuse University
Syracuse, NY 13244-4100 (USA)
Fax: (+1) 315-443-4070
E-mail: jtsperce@syr.edu

[**] We thank the National Science Foundation (Grant Nos. CHE-9521572 and 05-27898), the Donors of the Petroleum Research Fund as administered by the American Chemical Society, the Industrial Affiliates Program of the Center for Molecular Electronics, and Syracuse University for support of this work.

Supporting information for this article is available on the WWW under <http://www.wiley-vch.de/home/angewandte/> or from the author.